Characterization of Capacity and Outage of RIS-aided Downlink Systems under Rician Fading

Kali Krishna Kota, Praful D. Mankar, and Harpreet S. Dhillon

***Abstract*—This letter presents optimal beamforming and outage analysis for a Reconfigurable Intelligent Surface (RIS)-aided multiple input single output downlink system under Rician fading along both the direct and the RIS-assisted indirect links. We focus on maximizing the capacity for two transmitter architectures: fully digital (FD) and fully analog (FA). This capacity maximization problem with optimally configured RIS is shown to be L_1 norm-maximization with respect to the transmit beamformer. To obtain the optimal FD beamformer, we propose a complex L_1-principal component analysis (PCA)-based algorithm which has low computational complexity. We also propose a low-complexity optimal beamforming algorithm to obtain the FA beamforming solution. Further, we derive analytical upper bounds on the SNR achievable by the proposed algorithms and utilize them to characterize the lower bounds on outage probabilities. The derived bounds are numerically shown to closely match the achievable performance for a low-rank channel matrix and are shown to be exact for a unit-rank channel matrix.**

***Index Terms*—Reconfigurable intelligent surfaces, beamforming, outage probability, capacity, L1 norm.**

I. Introduction

RECONFIGURABLE intelligent surfaces (RISs) have attracted significant attention in recent years because of their ability to partially control the propagation environment and hence improve the performance of communications systems [1]–[4]. An extensive literature survey on the design of beamformers/precoders for RIS-aided multiple input single output/multiple input multiple output (MISO/MIMO) communication systems maximizing capacity is available in [5]–[7]. A key shortcoming of the prior art in this direction is the lack of analytical performance characterization of the proposed solutions, especially for multi antenna systems, which is the main inspiration behind this paper. There are just a handful of works focusing on the characterization of capacity and outage performance, *albeit* under simplistic settings, which we discuss below. For RIS-aided single input single output (SISO) systems, the authors of [8]–[14] analyze the outage probability with/without the presence of a direct link (DL) between the transmitter and receiver in various fading environments. In particular, asymptotic outage probability is derived for Rayleigh fading in [8] and [9] and for Rician fading in [10] in the presence of only the RIS-assisted indirect link (IL), which is further used to analyze the diversity order and asymptotic symbol error rate. The authors of [11] derived a closed-form expression for the outage with Rayleigh fading along both DL and IL. Next, [12] extended the result presented in [11] for Rician fading along IL. For similar settings, [13], [14] derived upper bounds on the outage, and [14] obtained the asymptotically exact outage in closed form. Furthermore, [15] have derived outage for RIS-aided fluid antenna systems.

In addition, few works focused on outage analysis for RIS-aided MISO systems. For example, [16] and [17] derived outage probabilities under various channel models for a maximum ratio transmission (MRT)-based transmit beamformer and optimally configured RIS phase shifts. The authors of [16] considered the line-of-sight (LoS)-Rayleigh channel model along IL, whereas [17] considered LoS-Rician channel along IL and Rician channel along DL. On the other hand, [18] analyzed the capacity of the MRT-based transmit beamformer and optimally configured discrete RIS phase shifts for a millimeter wave channel. Next, [19] presented statistically optimal beamforming for maximizing the ergodic capacity upper bound under Rician fading along both DL and IL and also characterized its outage performance. Finally, the ergodic capacity performance of a RIS-aided MIMO system with no DL is investigated in [20]. Particularly, they derived a closed-form expression of the channel gain distribution under Rayleigh-Rician fading along IL under full-rank and low-rank channel scenarios and utilized it to obtain ergodic capacity.

The above-mentioned works conventionally consider simplistic scenarios like SISO, Rayleigh channel, absence of a DL, LoS channel for BS-RIS link, etc. to facilitate tractable outage analysis. However, one of the main reasons to employ RIS is to provide an alternate BS-user link that includes strong LoS components for enhancing network coverage. Thus, it is more meaningful to consider Rician fading for outage analysis of RIS-aided networks, which is the main focus of this letter. A key challenge in analyzing the outage performance of RIS-aided multi-antenna systems is to accurately account for the impact of optimally configured RIS phase shifts and the transmit beamformer. In such a system, the optimal beamforming solution is usually obtained through complex iterative algorithms, which complicates further analysis. To handle this issue and obtain insights into the outage performance, we have obtained an upper bound on maximum SNR (or capacity) after optimal RIS configuration for a MISO system with two types of transmitter architectures, namely fully analog (FA) and fully digital (FD). Next, we derive the moment generating function (MGF) of this upper bounded SNR, which is then utilized to determine the outage probability lower bound. Interestingly, for an optimally configured RIS, we demonstrate that the SNR maximization with respect to the FD beamformer can be formulated as a complex L_1-norm PCA problem. Leveraging

K.K. Kota and P. D. Mankar are with Signal Processing and Communication Research Center, IIIT Hyderabad, India. (Email: kali.kota@research.iiit.ac.in, praful.mankar@iiit.ac.in). H. S. Dhillon is with Wireless@VT, Department of ECE, Virginia Tech, Blacksburg, VA (Email: hdhillon@vt.edu). The work of H. S. Dhillon was supported by the U.S. National Science Foundation under Grants ECCS-2030215 and CNS-2225511.

this, we present a low-complexity optimal digital beamforming algorithm for RIS-aided MISO systems.

II. System Model

This letter considers a RIS-aided MISO system with a single antenna user, wherein the transmitter is equipped with M antennas, and RIS comprises N reflecting elements. We consider two types of transmitter configurations: 1) *FD architecture*, where each antenna is connected to the baseband processing unit (BBU) via a dedicated radio frequency (RF) chain, and 2) *FA architecture*, where all the antennas are connected to the BBU via a single RF chain. We consider Rician faded DL and IL, and thus model BS-RIS, RIS-user, and BS-user links as

$$\mathbf{H} = \kappa_{l1}\bar{\mathbf{H}} + \kappa_{n1}\tilde{\mathbf{H}},\ \mathbf{h} = \kappa_{l2}\bar{\mathbf{h}} + \kappa_{n2}\tilde{\mathbf{h}} \text{ and } \mathbf{g} = \kappa_{l0}\bar{\mathbf{g}} + \kappa_{n0}\tilde{\mathbf{g}},$$

respectively, where $\kappa_{li} = \sqrt{\frac{K_i}{1+K_i}}$ and $\kappa_{ni} = \sqrt{\frac{1}{1+K_i}}$. Moreover, the tuple $\{K_0, \bar{\mathbf{g}}, \tilde{\mathbf{g}}\}$, $\{K_1, \bar{\mathbf{H}}, \tilde{\mathbf{H}}\}$, $\{K_2, \bar{\mathbf{h}}, \tilde{\mathbf{h}}\}$ consist of the Rice fading factor, LoS component, and multipath component associated with the BS-user, BS-RIS, and RIS-user links, respectively. We assume all fading factors are identical and therefore omit the subscript i from K_i, κ_{li}, and κ_{ni} from this point onward. Further, we model the LoS components as

$$\bar{\mathbf{g}} = \mathbf{a}_M(\theta_{\mathrm{bd}}^{\mathrm{d}}),\ \bar{\mathbf{h}} = \mathbf{a}_N(\theta_{\mathrm{rd}}),\ \text{and } \bar{\mathbf{H}} = \mathbf{a}_N(\theta_{\mathrm{ra}})\mathbf{a}_M(\theta_{\mathrm{bd}}^{\mathrm{i}})^T,$$

where $\mathbf{a}_L(\theta) = [1,\ e^{\frac{-j\pi d\cos(\theta)}{\lambda}}, \cdots,\ e^{\frac{-j\pi d\cos(\theta)}{\lambda}(L-1)}]^T$ is the array response of length L, and $\theta_{\mathrm{bd}}^{\mathrm{d}}$, $\theta_{\mathrm{bd}}^{\mathrm{i}}$, θ_{rd} are the angles of departure of the LoS components along the BS-user, BS-RIS, and RIS-user links, respectively, and θ_{ra} is the arrival angle at the RIS from BS. The multipath components are modeled as $\tilde{\mathbf{g}} \sim \mathcal{CN}(0, \mathbf{I}_M)$, $\tilde{\mathbf{h}} \sim \mathcal{CN}(0, \mathbf{I}_N)$, and $\tilde{\mathbf{H}}_{:,i} \sim \mathcal{CN}(0, \mathbf{I}_N)$.

The received signal at the user is

$$y = l(d_1, d_2)\mathbf{h}^T\mathbf{\Phi}\mathbf{H}\mathbf{f}x + l(d_0)\mathbf{g}^T\mathbf{f}x + n, \tag{1}$$

where $x \in \mathbb{C}$ is the transmit symbol with $\mathbb{E}[xx^*] = P_s$. Here, P_s is the total power available at the transmitter, $\mathbf{f} \in \mathbb{C}^M$ is the transmit beamforming vector, $\mathbf{\Phi} = \mathrm{diag}(\boldsymbol{\psi})$ is the RIS phase shift matrix, $l(d_1, d_2) = (d_1 d_2)^{-\alpha/2}, l(d_0) = d_0^{-\alpha/2}$ are the path loss models along IL and DL, respectively, d_0, d_1, d_2 are the distances between BS-user, BS-RIS, and RIS-user, respectively, α is the path loss exponent, and $n \sim \mathcal{CN}(0, \sigma_n^2)$ is the complex Gaussian noise. Further, the transmit beamforming vector belongs to 1) $\mathcal{B} = \{\mathbf{f} \in \mathbb{C}^M : \|\mathbf{f}\|_2 = 1\}$ under FD architecture to limit power consumption beyond the total available power and 2) $\mathcal{L} = \{\mathbf{f} \in \mathbb{C}^M : |\mathbf{f}_m| = 1/\sqrt{M}\}$ under the FA architecture, implying the unit modulus constraint. Next, $\boldsymbol{\psi} \in \mathbb{C}^N$ is the RIS phase shift vector with a unit amplitude constraint, i.e., $|\boldsymbol{\psi}_k| = 1$, to satisfy the passive RIS assumption. For given $\mathbf{f}$ and $\boldsymbol{\psi}$, received SNR is

$$\Gamma(\mathbf{f}, \boldsymbol{\psi}) = \gamma|\boldsymbol{\psi}^T\mathrm{diag}(\mathbf{h})\mathbf{H}\mathbf{f} + \mu\mathbf{g}^T\mathbf{f}|^2, \tag{2}$$

where $\gamma = \frac{P_s(d_1 d_2)^{-\alpha}}{\sigma_n^2}$ and $\mu = (\frac{d_0}{d_1 d_2})^{-\alpha/2}$ is the path loss ratio. The capacity maximization problem to obtain the jointly optimal transmit beamformer $\mathbf{f}$ and RIS phase shifts $\boldsymbol{\psi}$ is

$$\max_{\mathbf{f}, \boldsymbol{\psi}}\ \log_2(1 + \Gamma(\mathbf{f}, \boldsymbol{\psi})), \tag{3a}$$

$$\text{s.t. } \mathbf{f} \in \begin{cases} \mathcal{B}\ ; & \text{FD architecture} \\ \mathcal{L}\ ; & \text{FA architecture} \end{cases}, \tag{3b}$$

$$|\boldsymbol{\psi}_k| = 1;\ \forall k = 1, \ldots, N, \tag{3c}$$

where (3b) and (3c) represent the constraints on the transmit beamforming (FA/FD) and RIS phase shift vector, respectively. To evaluate the performance of the joint beamforming and RIS phase shift solution under both the architectures, we evaluate the *outage probability* defined as the probability that the received SNR is below threshold β and is given by

$$\mathrm{P}_{\mathrm{out}} = \mathbb{P}[\Gamma(\mathbf{f}_{\mathrm{opt}}, \boldsymbol{\psi}_{\mathrm{opt}}) < \beta]. \tag{4}$$

III. Optimal Beamforming

This section presents joint transmit beamformer and RIS phase shift solution to problem (3). Specifically, we aim to find maximum SNR in closed form for perfect CSI assumption.

A. Optimal RIS phase shifts

In this subsection, we obtain the optimal RIS phase shift matrix that maximizes the capacity (3a) for a given transmit beamforming vector $\mathbf{f}$. Since logarithm is a monotonically increasing function, maximizing capacity is equivalent to maximizing the SNR. For this, we rewrite (2) as

$$\Gamma(\mathbf{f}, \boldsymbol{\psi}) = \gamma|\boldsymbol{\psi}^T\mathbf{E}\mathbf{f} + \mu\mathbf{g}^T\mathbf{f}|^2, \tag{5}$$

where $\mathbf{E} = \mathrm{diag}(\mathbf{h})\mathbf{H}$. The received SNR can be maximized by co-phasing the fading coefficients using $\boldsymbol{\psi}$ to maximize the magnitude. Thus, for a given $\mathbf{f}$, the optimal RIS phase shift vector is

$$\boldsymbol{\psi}^{\mathrm{opt}} = \exp(-\angle\mathbf{E}\mathbf{f} + \angle\mathbf{g}^{\mathrm{T}}\mathbf{f}). \tag{6}$$

B. Optimal Transmit Beamforming

In the following subsections, we solve the optimal transmit beamforming problem under FD and FA architectures.

1) Digital Beamformer: For a given RIS phase shift vector $\boldsymbol{\psi}$, we can employ the MRT beamformer to maximize the SNR given in (5). However, the MRT beamformer and RIS phase shifts given in (6) need to be solved iteratively to arrive at the jointly optimal beamforming solution because of the coupled nature of these variables. On the contrary, in the following, we provide a novel approach to decouple these variables and provide a jointly optimal solution. Let $\mathbf{f}_{\mathrm{D}} = \mathbf{f}$ and $\mathbf{G} = \begin{bmatrix}\mathbf{E} & \mu\mathbf{g}^T\end{bmatrix}^T$ be a matrix concatenated with DL and IL channel matrices. Substituting (6), we can rewrite (5) as

$$\Gamma(\mathbf{f}_{\mathrm{D}}, \boldsymbol{\psi}^{\mathrm{opt}}) = (\|\mathbf{E}\mathbf{f}_{\mathrm{D}}\|_1 + \mu\|\mathbf{g}\mathbf{f}_{\mathrm{D}}\|_1)^2 = \|\mathbf{G}\mathbf{f}_{\mathrm{D}}\|_1^2. \tag{7}$$

It can be seen from (7) that the capacity maximization problem (3) with optimal $\boldsymbol{\psi}^{\mathrm{opt}}$ reduces to the selection of the transmit beamforming vector $\mathbf{f}_{\mathrm{D}}$ that maximizes the L_1 norm of $\mathbf{G}\mathbf{f}_{\mathrm{D}}$. The L_1 norm maximization problem (7) to obtain the optimal transmit beamformer for FD architecture is defined as

$$\max_{\|\mathbf{f}_{\mathrm{D}}\|_2 = 1} \|\mathbf{G}\mathbf{f}_{\mathrm{D}}\|_1. \tag{8}$$

In essence, the transmit beamformer problem has now effectively reduced to estimating L_1 principal components of the concatenated channel matrix $\mathbf{G} = [(\mathrm{diag}(\mathbf{h})\mathbf{H})^T\mu\mathbf{g}]^T$. To solve this, we employ a novel approach proposed in [21] that breaks such a complex L_1 PCA problem into two independent tractable optimization problems that can be solved iteratively.

The L_1 norm of $\mathbf{G}\mathbf{f}_{\mathrm{D}}$ can be represented from [21] as

$$\|\mathbf{G}\mathbf{f}_{\mathrm{D}}\|_1 = \max\nolimits_{\mathbf{u}\in\mathcal{U}^{N+1}} \mathrm{Re}\{\mathbf{u}^H\mathbf{G}\mathbf{f}_{\mathrm{D}}\},$$

where $\mathcal{U}^{N+1} \triangleq \{\mathbf{u}\in\mathbb{C}^{N+1} : |\mathbf{u}_i| = 1; \forall i\}$ is a unimodular vector space and $\mathbf{u}^{\mathrm{opt}} = \exp(-\angle\mathbf{G}\mathbf{f}_{\mathrm{D}})$. Thus, (8) becomes

$$\begin{aligned}\max_{\|\mathbf{f}_{\mathrm{D}}\|_2=1} \|\mathbf{G}\mathbf{f}_{\mathrm{D}}\|_1 &= \max_{\|\mathbf{f}_{\mathrm{D}}\|_2=1} \max_{\mathbf{u}\in\mathcal{U}^{N+1}} \mathrm{Re}\{\mathbf{u}^H\mathbf{G}\mathbf{f}_{\mathrm{D}}\},\\ &\overset{(a)}{=} \max_{\mathbf{u}\in\mathcal{U}^{N+1}} \max_{\|\mathbf{f}_{\mathrm{D}}\|_2=1} \mathrm{Re}\{\mathbf{u}^H\mathbf{G}\mathbf{f}_{\mathrm{D}}\}, \quad (9)\end{aligned}$$

where Step (a) follows from the fact that the maximization operators can be exchanged for the linear objective. For a fixed $\mathbf{u}$, the optimal transmit beamformer becomes

$$\mathbf{f}_{\mathrm{D}}^{\mathrm{opt}} = \mathbf{G}^H\mathbf{u}/\|\mathbf{G}^H\mathbf{u}\|. \quad (10)$$

Thus, RHS of (9) becomes $\max_{\mathbf{u}\in\mathcal{U}^{N+1}} \mathrm{Re}\{\mathbf{u}^H\mathbf{G}\mathbf{f}^{\mathrm{opt}}\}$ which is maximized by $\mathbf{u}$ as

$$\mathbf{u}^{\mathrm{opt}} = \exp\left(-\angle\mathbf{G}\mathbf{f}_{\mathrm{D}}^{\mathrm{opt}}\right). \quad (11)$$

Finally, the optimal beamformer $\mathbf{f}_{\mathrm{D}}^{\mathrm{opt}}$ can be obtained by evaluating (10) and (11) iteratively untill (8) converges as shown in Algorithm 1. In summary, the algorithm first maximizes the SNR (expressed in L_1 norm) by employing complex L_1-PCA-based method to obtain the optimal beamformer $\mathbf{f}_{\mathrm{D}}^{\mathrm{opt}}$. Recall that this form of SNR is obtained after maximizing SNR w.r.t. $\boldsymbol{\psi}$ for a given $\mathbf{f}_{\mathrm{D}}$. Thus, we update $\boldsymbol{\psi}$ for optimal beamformer $\mathbf{f}_{\mathrm{D}}^{\mathrm{opt}}$ to obtain a jointly optimal solution. Algorithm 1 has a complexity of $\mathcal{O}(NM)$ per iteration and is guaranteed to converge to optimal solution; please refer to [21] for details. Further, it can be seen numerically that Algorithm 1 converges faster than the widely used MRT-based solution.

Algorithm 1: Digital Beamforming Algorithm

Input: $\mathbf{g}$, $\mathbf{E}$ and $\mathbf{G}$.
Initialization: $\mathbf{u}, \mathbf{f}_{\mathrm{D}}$
Repeat
  $\mathbf{f}_{\mathrm{D}} = \frac{\mathbf{G}^H\mathbf{u}}{\|\mathbf{G}^H\mathbf{u}\|}$,
  $\mathbf{u} = \exp(-\angle\mathbf{G}\mathbf{f}_{\mathrm{D}})$,
Untill: $\mathrm{Re}\{\mathbf{u}^H\mathbf{G}\mathbf{f}_{\mathrm{D}}\}$ **converges**;
$\mathbf{f}_{\mathrm{D}}^{\mathrm{opt}} = \mathbf{f}_{\mathrm{D}}$ and $\boldsymbol{\psi}^{\mathrm{opt}} = \exp(-\angle\mathbf{E}\mathbf{f}_{\mathrm{D}}^{\mathrm{opt}} + \angle\mathbf{g}^{\mathrm{T}}\mathbf{f}_{\mathrm{D}}^{\mathrm{opt}})$.

2) Analog Beamformer: The transmit beamformer under FA architecture is obtained by maximizing SNR as

$$\max_{|\mathbf{f}_{\mathrm{A,m}}|=\frac{1}{\sqrt{M}}} |(\boldsymbol{\psi}^T\mathbf{E} + \mu\mathbf{g}^T)\mathbf{f}_{\mathrm{A}}|^2, \quad (12)$$

where $\mathbf{f}_{\mathrm{A,m}}$ is the $m-\mathrm{th}$ element of analog beamformer $\mathbf{f}_{\mathrm{A}}$. Consequently, $\mathbf{f}_{\mathrm{A}}$ that maximizes (12) for a given $\boldsymbol{\psi}$ is

$$\mathbf{f}_{\mathrm{A}}^{\mathrm{opt}} = e^{-j(\angle\boldsymbol{\psi}^T\mathbf{E} - \angle\mathbf{g})}/\sqrt{M}. \quad (13)$$

However, the obtained closed-form expressions for $\mathbf{f}_{\mathrm{A}}$ and $\boldsymbol{\psi}$ in (13) and (6) (where $\mathbf{f} = \mathbf{f}_{\mathrm{A}}$), depend on each other. Hence, these solutions are iteratively evaluated until (12) converges as summarized in Algorithm 2. Algorithm 2 has a complexity of $\mathcal{O}(MN)$ per iteration, arising due to matrix multiplication in Steps 1 and 2. The performance characterization of such a RIS-aided system with FA architecture has not been investigated so far. Motivated by this, we study the capacity and outage performance as follows. We begin by simplifying the maximum achievable SNR for FA design using (7) as

Algorithm 2: Analog Beamforming Algorithm

Input: $\mathbf{g}$ and $\mathbf{E}$.
Initialization: $\mathbf{u}, \mathbf{f}_{\mathrm{A}}$
Repeat
  $\boldsymbol{\psi} = e^{-j(\angle\mathbf{E}\mathbf{f}_{\mathrm{A}} - \angle\mathbf{g})}$,
  $\mathbf{f}_{\mathrm{A}} = \frac{1}{\sqrt{M}} e^{-j(\angle\boldsymbol{\psi}^T\mathbf{E} - \angle\mathbf{g})}$,
Untill: $\Gamma(\mathbf{f}, \boldsymbol{\Phi})$ **converges**;
$\mathbf{f}_{\mathrm{A}}^{\mathrm{opt}} = \mathbf{f}_{\mathrm{A}}$ and $\boldsymbol{\psi}^{\mathrm{opt}} = \boldsymbol{\psi}$.

$$\max_{|\mathbf{f}_{\mathrm{A,m}}|=\frac{1}{\sqrt{M}}} \|\mathbf{G}\mathbf{f}_{\mathrm{A}}\|_1^2. \quad (14)$$

The above objective function can be upper-bounded as

$$\|\mathbf{G}\mathbf{f}_{\mathrm{A}}\|_1 = \sum_{n=1}^{N}\left|\sum_{m=1}^{M}\mathbf{G}_{nm}\mathbf{f}_{\mathrm{A,m}}\right| \overset{(a)}{\leq} \sum_{n=1}^{N}\sum_{m=1}^{M}\frac{|\mathbf{G}_{nm}|}{\sqrt{M}} = \frac{\|\mathbf{G}\|_{1,1}}{\sqrt{M}},$$

where $\|\cdot\|_{1,1}$ denotes the $L_{1,1}$ norm. Here, Step (a) follows from the triangle inequality ($|a+b| \leq |a|+|b|$) and the analog beamforming constraint $|\mathbf{f}_{\mathrm{A,m}}| = \frac{1}{\sqrt{M}}$. We summarize this upper bound in the following theorem.

Theorem 1. *The maximum capacity of a RIS-aided MISO communication system with FA architecture is upper bounded by* $\log_2(1+\Gamma^{\mathrm{UB}}) = \log_2(1+\frac{\gamma}{M}\|\mathbf{G}\|_{1,1}^2)$.

Corollary 1.1. *The maximum capacity upper bound of the RIS-aided MISO downlink given in Theorem 1 under both FA and FD architectures reduces to* $\log_2(1+\frac{\gamma}{M}\|\bar{\mathbf{G}}\|_{1,1}^2) = \log_2(1+(N+\mu)^2M\gamma)$ *for an LoS-channel.*

Proof: In the presence of an LoS channel, we have $\mathbf{g} = \kappa_l\bar{\mathbf{g}}$, $\mathbf{h} = \kappa_l\bar{\mathbf{h}}$, and $\mathbf{H} = \kappa_l\bar{\mathbf{H}}$, corresponding to $K = \infty$ in the Rician channel model discussed in Section II. Thus, matrix $\mathbf{G}$ becomes equal to $\bar{\mathbf{G}} = [(\mathrm{diag}(\bar{\mathbf{h}})\bar{\mathbf{H}})^{\mathrm{T}}\ \mu\bar{\mathbf{g}}]^{\mathrm{T}}$. For such a case, the channel envelope with optimal RIS phase shift $\boldsymbol{\psi}_{\mathrm{opt}}$ (7), and a given FA beamformer $\mathbf{f}_{\mathrm{A}}$ becomes

$$\begin{aligned}\|\bar{\mathbf{G}}\mathbf{f}_{\mathrm{A}}\|_1 &= \sum\nolimits_{n=1}^{N+1}\big|\sum\nolimits_{m=1}^{M}\bar{\mathbf{G}}_{nm}\mathbf{f}_{\mathrm{A,m}}\big|,\\ &\overset{(a)}{=} \sum\nolimits_{n=1}^{N+1}\big|\sum\nolimits_{m=1}^{M}\bar{\mathbf{G}}_{n1}c_m\mathbf{f}_{\mathrm{A,m}}\big|,\\ &\overset{(b)}{=} \frac{1}{\sqrt{M}}\sum\nolimits_{n=1}^{N+1}\sum\nolimits_{m=1}^{M}|\bar{\mathbf{G}}_{n1}|,\\ &\overset{(c)}{=} (N+\mu)\sqrt{M}, \quad (15)\end{aligned}$$

where Step (a) follows from the fact that the columns of matrix $\bar{\mathbf{G}}$ are linearly dependent, Step (b) follows from the unit modulus constraint on the analog beamformer $\mathbf{f}_{\mathrm{A}}$ such that it maximizes the sum by setting $\mathbf{f}_{\mathrm{A,m}} = \frac{1}{\sqrt{M}}c_m^H$ and the fact that $|c_m| = 1$, and Step (c) follows from $|\bar{\mathbf{G}}_{n1}| = 1$.

Moreover, the equality presented in (15) also holds for digital beamforming. This is because the inner summation given in Step (b) is also maximized for the digital beamformer $\mathbf{f}_{\mathrm{D,m}} = \frac{1}{\sqrt{M}}c_m^H$ such that $\|\mathbf{f}_{\mathrm{D}}\|^2 = 1$. ■

Corollary 1.2. *The upper bound given in Corollary 1.1 is achievable by both FD and FA architectures in the absence of DL under dominant LoS and is given by* $\log_2(1+\gamma N^2M)$.

Proof. Let $\bar{\mathbf{E}} = \text{diag}(\bar{\mathbf{h}})\bar{\mathbf{H}}$. Thus, the SNR given in (7) in the absence of DL under dominant LoS channel becomes

$$\gamma\|\bar{\mathbf{E}}\mathbf{f}\|_1^2 = \gamma\|\text{diag}(\mathbf{a}_N(\theta_{\text{rd}}))\mathbf{a}_N(\theta_{\text{ra}})\|_1^2|\mathbf{a}_M(\theta_{\text{bd}}^i)^T\mathbf{f}|^2.$$

The optimal choice of $\mathbf{f}$ under the FA and FD architectures is $\mathbf{f}_{\text{A}}^{\text{opt}} = e^{-j\angle\mathbf{a}_M(\theta_{\text{bd}}^i)}/\sqrt{M}$ and $\mathbf{f}_{\text{D}}^{\text{opt}} = \mathbf{a}_M^H(\theta_{\text{bd}}^i)/\|\mathbf{a}_M^H(\theta_{\text{bd}}^i)\|$, respectively. For these optimal choices, the SNR becomes

$$\gamma\|\bar{\mathbf{E}}\mathbf{f}^{\text{opt}}\|_1^2 = \gamma N^2 M, \quad \text{for } \mathbf{f}^{\text{opt}} \in \{\mathbf{f}_{\text{A}}^{\text{opt}}, \mathbf{f}_{\text{D}}^{\text{opt}}\}.$$

Thus, it can be seen that the upper bound proposed in Corollary 1.1 is achievable by both the architectures in a LoS dominated scenario without DL. □

Remark 1. *From Corollary 1.2, it can be safely deduced that the capacity upper bound presented in Theorem 1 becomes tight in the absence of DL (i.e., $\mathbf{G} = \mathbf{E}$) under scenarios including strong LoS components (i.e., for a large K). In other words, the capacity upper bound in the absence of DL becomes tighter as the rank of $\mathbf{E}$ becomes low, which further reduces to equality when $\mathbf{E}$ becomes unit rank, i.e., $K \to \infty$. Moreover, the capacity upper bound in the presence of DL can also be achieved when the angle between DL and IL is very small and K is large (in which case $\mathbf{G}$ becomes unit rank).*

IV. Outage Probability Analysis

The outage performance characterization of RIS-aided FD/FA systems in the absence of DL is as follows. The outage probability defined in (4) is lower bounded as

$$\text{P}_{\text{out}} \geq \text{P}_{\text{out}}^{\text{LB}} = \mathbb{P}\left[\Gamma^{\text{UB}} \leq \beta\right]. \tag{16}$$

Using Theorem 1, the SNR upper bound in the absence of DL becomes $\Gamma^{\text{UB}} = \gamma\|\mathbf{E}\|_{1,1}^2$. Thus, we can write

$$\text{P}_{\text{out}}^{\text{LB}} = \mathbb{P}\left[\|\mathbf{E}\|_{1,1} \leq \sqrt{\beta/\gamma}\right]. \tag{17}$$

Recall that the above lower bound becomes tighter for a low-rank channel matrix $\mathbf{E}$, which further reduces to equality for $\mathbf{E}$ with rank 1 as highlighted in Remark 1. Note that $\|\mathbf{E}\|_{1,1}$ is the sum-of-product of Rician random variables, making it difficult to derive outage probability directly. Thus, we first obtain its MGF and then use it to determine $\text{P}_{\text{out}}^{\text{LB}}$.

Theorem 2. *The MGF of $\|\mathbf{E}\|_{1,1}$ is*

$$M(-s) = s^{MN}\left[\int_0^\infty g(h)^M f_{|\mathbf{h}_n|}(h)\text{d}h\right]^N, \tag{18}$$

where $g(h) = \mathcal{L}\left(1 - Q_1\left(\frac{\kappa_l}{\kappa_n}, \frac{x}{|\mathbf{h}_n|\kappa_n}\right)\right)$, $Q_1(\cdot)$ is the Marcum-Q function, $\mathcal{L}(\cdot)$ is Laplace transform (LT), and $f(\cdot)$ is Rician density function.

Proof: Let $Y_n = |\mathbf{h}_n|\sum_{m=1}^M |\mathbf{H}_{nm}|$ and let us define

$$Y = \|\mathbf{E}\|_{1,1} = \sum\nolimits_{n=1}^N Y_n. \tag{19}$$

We begin by writing the MGF of the channel gain $|\mathbf{H}_{nm}|$ by using the differentiation property of LT as

$$M_{|\mathbf{H}_{nm}|}(-s) = s\mathcal{L}(F_{|\mathbf{H}_{nm}|}(x)),$$

where $\mathcal{L}(\cdot)$ represents LT and $F_{|\mathbf{H}_{nm}|}(x) = 1 - Q_1(\frac{\kappa_l}{\kappa_n}, \frac{x}{\kappa_n})$ is the cumulative distribution function (CDF) of $|\mathbf{H}_{nm}|$. Let $X_n = \sum_{m=1}^M |\mathbf{H}_{nm}|$. The n-th term of Y given in (19) becomes $Y_n = |\mathbf{h}_n|X_n$ and thus its CDF is determined as

$$\begin{aligned} F_{Y_n}(y) &= \int_0^\infty \int_0^{\frac{y}{|\mathbf{h}_n|}} f_{|\mathbf{h}_n|}(h) f_{X_n}(x)\text{d}x\text{d}h, \\ &= \int_0^\infty f_{|\mathbf{h}_n|}(h) F_{X_n}(y/h)\text{d}h. \end{aligned} \tag{20}$$

Thus, the MGF of Y_n can be obtained as

$$\begin{aligned} M_{Y_n}(-s) &= s\mathcal{L}\left(F_{Y_n}(y)\right), \\ &\overset{(a)}{=} \int_0^\infty f_{|\mathbf{h}_n|}(h) s\mathcal{L}(F_{X_n}(y/h))\text{d}h, \\ &\overset{(b)}{=} \int_0^\infty f_{|\mathbf{h}_n|}(h)\left[s\mathcal{L}\left(1 - Q_1(\kappa_l/\kappa_n, y/(h\kappa_n))\right)\right]^M \text{d}h. \end{aligned}$$

where Step (a) follows from using (20) and the fact that LT is a linear operator, Step (b) follows from $M_{X_n}(-s) = s\mathcal{L}(F_{X_n}(x))$ and using the fact that $\mathbf{H}_{nm}$ are independent and identically distributed (i.i.d.) random variables. Since $Y_n;\ \forall n$ are i.i.d. random variables, we can obtain the MGF of Y as $M_Y(s) = M_{Y_n}(s)^N$. This completes the proof. ■

Finally, we evaluate the lower bound on the outage probability as $\text{P}_{\text{out}}^{\text{LB}} = \mathcal{L}^{-1}\left\{\frac{M(-s)}{s}\right\}$, where $M(s)$ is MGF of $\|\mathbf{E}\|_{1,1}$ and is given in Theorem 2. For inverting the MGF, we employ a widely used numerical inversion technique given in [22].

V. Numerical Results and Discussion

This section presents the numerical analysis of capacity and outage obtained by the proposed algorithms for FD/FA architectures and compares them with the upper bound derived in Theorem 1. For numerical analysis, we assume the number of BS antennas $M = 4$, the number of RIS elements $N = 64$, path loss ratio $\mu = 5$ dB, and $\gamma = 1$. Figure 1 (a) shows the capacity as a function of N under both FD and FA architectures. It can be observed that the capacity increases with N as well as with the Rician factor K. This is expected as larger N provides larger array gains and larger K provides stronger LoS paths, ensuring better capacities. Further, it can be seen that the capacity is close to the derived upper bound for reasonable values of K which further becomes tight with increasing K. This is because the LoS component dominates the channel for very large K, and the upper bound reduces to equality for the LoS channel as mentioned in Corollary 1.1. Besides, we can also observe that the AB and DB perform almost equally as K becomes larger.

Figure 1 (b) shows the comparison of achievable capacity under three schemes, namely 1) the absence of DL at $\mu = -\infty$, 2) the presence of DL at $\mu = 10$ and 20 dB, and 3) absence of RIS, i.e., IL. We first observe that the derived upper bound is tight in all the schemes, especially when K is large. Next, we see that the capacity improves with μ, which strengthens DL, which in turn provides additional spatial diversity to achieve a higher capacity. However, it is noteworthy that the capacity improves slowly with an increase in N when μ is large. This is because, in the presence of strong DL, the improvement in receive SNR due to RIS is not significant. Thus, as capacity is a logarithmic function of SNR, we observe a saturation in capacity with N. Another interesting observation at large μ and increasing N shows the proposed

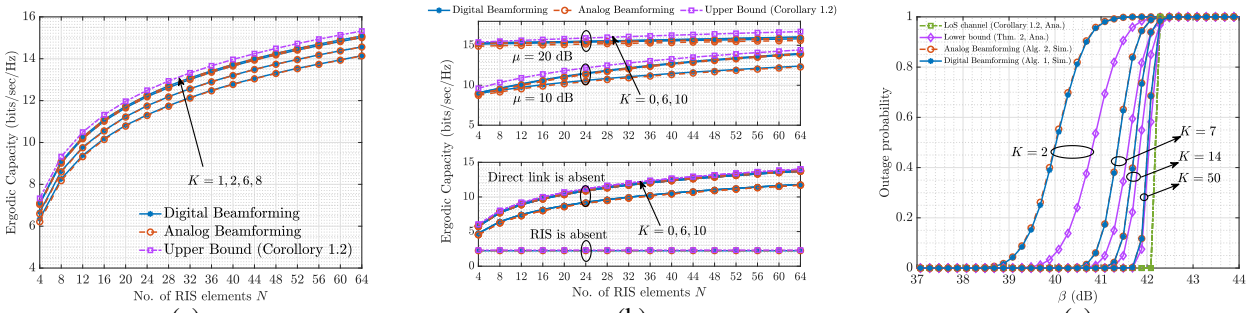

Fig. 1: Capacity vs. N without DL (a), with DL or IL (b, bottom), and with both DL and IL (b, top). Outage probability (c).

capacity upper bound becoming loose. This is because, the concatenated matrix $\mathbf{G} = [\mathbf{E}^T \mu \mathbf{g}^T]^T$ becomes rank 2 at large values of μ, even in a dominant LoS propagation scenario. In summary, this figure verifies that the upper bound derived in Corollary 1.1 becomes achievable and reduces to as given in Corollary 1.2 when μ decreases and K increases (i.e., when DL is weak and IL contains strong LoS).

Figure 1 (c) shows the outage performance of the proposed beamforming schemes under FA and FD architectures in the absence of DL at various values of K. We first observe that the outage performance of both architectures is very close. As K increases, these performances increasingly approach the derived outage lower bound presented in Section IV. It can also be observed that the distributions of exact SNR under both the architectures and the SNR upper bound converge to the deterministic value derived in Corollary 1.2, i.e. $\Gamma(\mathbf{f}^{\text{opt}}, \psi^{\text{opt}}) = \Gamma^{\text{UB}} = \gamma M N^2$ as $K \to \infty$.

VI. Conclusion

This letter investigated optimal beamforming for maximizing the capacity of RIS-aided downlink systems with FD and FA architectures in the presence of Rician faded DL and IL. We first showed that the capacity maximization problem reduces to an L_1-norm maximization problem with respect to the transmit beamformer after optimally configuring the RIS. We proposed a complex L_1-PCA-based algorithm to obtain the optimal FD beamformer. We proposed another algorithm to obtain the optimal FA beamformer with low complexity. Both the proposed algorithms iterate over two closed-form expressions. To characterize the performance of the proposed algorithms, we derived an upper bound on the capacity and analyzed its corresponding outage performance. Specifically, we derived the MGF of the envelope of the SNR upper bound, which we then numerically inverted to obtain the outage probability lower bound. Moreover, we analytically established that the proposed bounds on capacity and outage become exact when the channel matrix becomes unit rank, i.e., LoS components of DL and IL are strong and aligned.

References

[1] E. Basar, M. Di Renzo, J. De Rosny, M. Debbah, M.-S. Alouini, and R. Zhang, "Wireless communications through reconfigurable intelligent surfaces," *IEEE Access*, vol. 7, pp. 116 753–116 773, 2019.

[2] Y. Liu, X. Liu, X. Mu, T. Hou, J. Xu, M. Di Renzo, and N. Al-Dhahir, "Reconfigurable intelligent surfaces: Principles and opportunities," *IEEE Commun. Surveys & Tuts.*, vol. 23, no. 3, pp. 1546–1577, 2021.

[3] M. Di Renzo, F. H. Danufane, and S. Tretyakov, "Communication models for reconfigurable intelligent surfaces: From surface electromagnetics to wireless networks optimization," *Proc. IEEE*, vol. 110, no. 9, pp. 1164–1209, 2022.

[4] K. Zhong, J. Hu, C. Pan, M. Deng, and J. Fang, "Joint waveform and beamforming design for RIS-aided ISAC systems," *IEEE Signal Processing Letters*, vol. 30, pp. 165–169, 2023.

[5] J. Wang, H. Wang, Y. Han, S. Jin, and X. Li, "Joint transmit beamforming and phase shift design for reconfigurable intelligent surface assisted MIMO systems," *IEEE Trans. Cogn. Commun. Netw.*, vol. 7, no. 2, pp. 354–368, 2021.

[6] A. L. Moustakas, G. C. Alexandropoulos, and M. Debbah, "Capacity optimization using reconfigurable intelligent surfaces: A large system approach," in *IEEE GLOBECOM*, 2021.

[7] J. Choi, G. Kwon, and H. Park, "Multiple intelligent reflecting surfaces for capacity maximization in LOS MIMO systems," *IEEE Wirel. Commun. Lett.*, vol. 10, no. 8, pp. 1727–1731, 2021.

[8] A.-A. A. Boulogeorgos and A. Alexiou, "Performance analysis of reconfigurable intelligent surface-assisted wireless systems and comparison with relaying," *IEEE Access*, vol. 8, pp. 94 463–94 483, 2020.

[9] D. Kudathanthirige, D. Gunasinghe, and G. Amarasuriya, "Performance analysis of intelligent reflective surfaces for wireless communication," in *IEEE ICC*, 2020.

[10] A. M. Salhab and M. H. Samuh, "Accurate performance analysis of reconfigurable intelligent surfaces over rician fading channels," *IEEE Wirel. Commun. Letters*, vol. 10, no. 5, pp. 1051–1055, 2021.

[11] T. Van Chien, L. T. Tu, S. Chatzinotas, and B. Ottersten, "Coverage probability and ergodic capacity of intelligent reflecting surface-enhanced communication systems," *IEEE Commun. Lett.*, vol. 25, no. 1, pp. 69–73, 2020.

[12] P. Xu, W. Niu, G. Chen, Y. Li, and Y. Li, "Performance analysis of ris-assisted systems with statistical channel state information," *IEEE Trans. Veh. Technol.*, vol. 71, no. 1, pp. 1089–1094, 2021.

[13] Q. Tao, J. Wang, and C. Zhong, "Performance analysis of intelligent reflecting surface aided communication systems," *IEEE Commun. Lett.*, vol. 24, no. 11, pp. 2464–2468, 2020.

[14] T. Wang, G. Chen, J. P. Coon, and M.-A. Badiu, "Chernoff bound and saddlepoint approximation for outage probability in IRS-assisted wireless systems," in *IEEE GLOBECOM Workshops*, 2021.

[15] F. R. Ghadi, K.-K. Wong, W. K. New, H. Xu, R. Murch, and Y. Zhang, "On performance of RIS-aided fluid antenna systems," *IEEE Wireless Communications Letters*, 2024.

[16] N. K. Kundu and M. R. McKay, "RIS-assisted MISO communication: Optimal beamformers and performance analysis," in *IEEE GLOBECOM Workshops*, 2020.

[17] C. Guo, Y. Cui, F. Yang, and L. Ding, "Outage probability analysis and minimization in intelligent reflecting surface-assisted MISO systems," *IEEE Commun. Lett.*, vol. 24, no. 7, pp. 1563–1567, 2020.

[18] J. Ye, A. Kammoun, and M.-S. Alouini, "Optimal phase shift solution and diversity analysis for discrete RIS-assisted systems under rank deficient channels," *IEEE Wirel. Commun. Lett.*, 2023.

[19] K. K. Kota, M. S. S. Manasa, P. D. Mankar, and H. S. Dhillon, "Statistically optimal beamforming and ergodic capacity for RIS-aided MISO systems," *IEEE Access*, pp. 1–1, 2023.

[20] M. Abbasi Mosleh, F. Heliot, and R. Tafazolli, "Ergodic capacity analysis of reconfigurable intelligent surface assisted MIMO systems over rayleigh-rician channels," *IEEE Commun. Lett.*, no. 1, pp. 75–79, 2023.

[21] N. Tsagkarakis, P. P. Markopoulos, G. Sklivanitis, and D. A. Pados, "L1-norm principal-component analysis of complex data," *IEEE Trans. Sig. Proc.*, vol. 66, no. 12, pp. 3256–3267, 2018.

[22] Y.-C. Ko, M.-S. Alouini, and M. K. Simon, "Outage probability of diversity systems over generalized fading channels," *IEEE Trans. Commun.*, vol. 48, no. 11, pp. 1783–1787, 2000.